CORA Cork Open Research Archive
Cartlann Taighde Oscailte Chorcaí

Title	GaAs filter/isolator using transmission-zero-generating unilateral frequency-selective stages
Authors	Li, Kexin;Psychogiou, Dimitra
Publication date	2026-03-10
Original Citation	Li, K & Psychogiou, D 2026, GaAs filter/isolator using transmission-zero-generating unilateral frequency-selective stages. in IMFW 2026 - IEEE MTT-S International Microwave Filter Workshop. IMFW 2026 - IEEE MTT-S International Microwave Filter Workshop, Institute of Electrical and Electronics Engineers Inc., pp. 1-3, 2026 IEEE MTT-S International Microwave Filter Workshop, IMFW 2026, Hong Kong, Hong Kong, 7/02/26. https://doi.org/10.1109/IMFW64610.2026.11419052
Type of publication	Conference item
Link to publisher's version	https://www.scopus.com/pages/publications/105035984652 - 10.1109/IMFW64610.2026.11419052
Rights	© 2026, IEEE. Personal use of this material is permitted. Permission from IEEE must be obtained for all other uses, in any current or future media, including reprinting/republishing this material for advertising or promotional purposes, creating new collective works, for resale or redistribution to servers or lists, or reuse of any copyrighted component of this work in other works.
Download date	2026-11-04 02:53:11
Item downloaded from	https://hdl.handle.net/10468/18715

UCC
University College Cork, Ireland
Coláiste na hOllscoile Corcaigh

GaAs Filter/Isolator Using Transmission-Zero-Generating Unilateral Frequency-Selective Stages

Kexin Li
Tyndall National Institute
University College Cork
Cork, Ireland
kexin.li@tyndall.ie

Dimitra Psychogiou
Tyndall National Institute
University College Cork
Cork, Ireland
dpsychogiou@ucc.ie

***Abstract*—A Ku-band GaAs monolithic microwave integrated circuit (MMIC) RF component that co-integrates the function of a quasi-elliptic bandpass filter and an RF isolator (BPFI) is reported. It is based on cascaded unilateral frequency-selective stages (UFSs) comprising a transistor-based path and multi-resonant feedback that introduces one pole and two transmission zeros (TZs). A coupled-resonator-based synthesis methodology is developed, extending conventional reciprocal filter synthesis to scalable UFS-based non-reciprocal filters. For experimental validation, a two-stage BPFI was manufactured using a 0.15-µm GaAs process. The prototype exhibits a quasi-elliptic response with center frequency of 15.9 GHz, a 3-dB fractional bandwidth of 20%, 60 dB directivity, and wide upper stopband shaped by four TZs and with greater than 20 dB rejection between DC to 12.4 GHz and 20.1 to 48.3 GHz (measured up to 38 GHz; simulated thereafter).**

***Keywords*—Isolator, monolithic microwave integrated circuit (MMIC), non-reciprocal filter, quasi-elliptic filter, RF co-design.**

I. Introduction

Unilateral components such as isolators and circulators play key roles in in-band full-duplex (IBFD) systems [1], where the demand for multi-functionality, low complexity, compactness, and high integration is ever increasing. To address these requirements, RF co-design methodologies have gained considerable attention, as they allow multiple RF processing functions to be consolidated into a single device, thereby reducing the footprint of the RF front-end. Among the various co-design strategies, the co-integration of RF filters with isolators or circulators is gaining significant attention, since it can simultaneously provide directional transmission, frequency selectivity, and interference suppression. To further strengthen the interference suppression capability of such co-integrated systems, transmission zeros (TZs) are highly desirable in the out-of-band response [2].

For the co-integration of bandpass filters and RF isolators (BPFIs), several approaches have been reported based on ferrite materials, spatiotemporally modulated (STM) resonators, and transistor-based configurations. Ferrite-based methods [3], while effective, require magnetic biasing and are incompatible with semiconductor technologies due to their bulk size and process incompatibility. STM resonators offer better IC compatibility but suffer from high insertion loss of 3.2–6.8 dB [4] and limited operating frequencies constrained by requirement of high modulation frequency. Transistor-based solutions [5] provide moderate gain (0–10 dB), but consume substantial power (~100 mW) and are typically

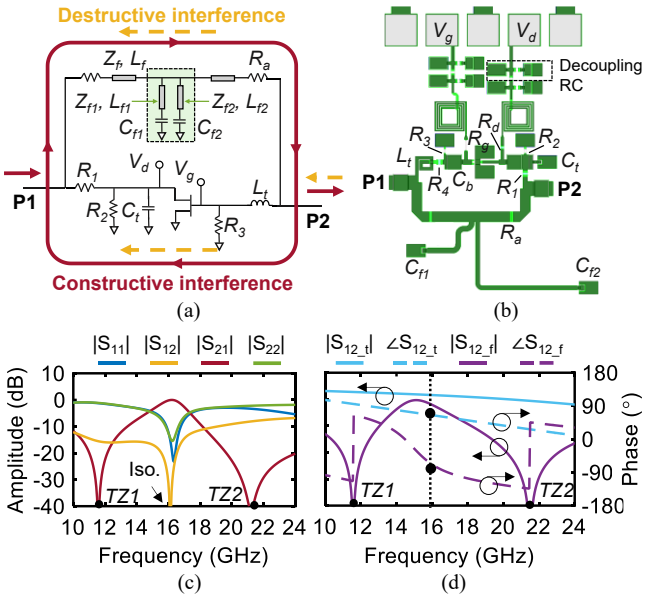


Fig. 1. (a) Circuit schematic [8] and (b) Layout of the MMIC UFS. Circuit-simulated S-parameters of (c) the UFS and (d) the transistor-based ($|S_{12_t}|$) and feedback ($|S_{12_f}|$) RF signal paths [8]. In (a), L_t =0.52 nH, C_t =0.23 pF, R_1 =37 Ω, R_2 =109 Ω, R_3 =239 Ω, R_a =1.7 Ω, $Z_{f\&f1\&f2}$=57 Ω, L_f =15°@16 GHz, L_{f1} =39°@16 GHz, L_{f2} =16°@16 GHz, C_{f1} =0.45 pF, C_{f2} =0.33 pF.

realized through circuit-level optimization rather than systematic synthesis methodologies. More recently, a novel class of unilateral frequency-selective stages (UFSs) has enabled the realisation of BPFI using conventional coupled-resonator synthesis techniques. These unilateral filters have demonstrated competitive RF performance in terms of gain (4.2–5.8 dB) and isolation (44–71 dB) [6]. Nevertheless, they are constrained by high power consumption (114–228 mW) and rely on passive stages for TZ generation, which require additional inverters for interconnection, increasing circuit size and design complexity [7]. To eliminate the need for passive stages in TZ generation, [8] introduced two TZs directly within the UFS, achieving symmetric selectivity; however, the resulting BPFI exhibits relatively low directivity (13–20 dB).

Building upon the concept in [8], this work presents an alternative BPFI design that employs two cascaded UFSs to realize a quasi-elliptic transfer function with higher directivity and selectivity than the prototype in [8]. Unlike [8], which utilizes one UFS and one passive resonator yielding two poles and two TZs, the proposed BPFI features a transfer function shaped by two poles and four TZs. By cascading UFSs with intentionally separated TZ positions, the proposed BPFI achieves higher directivity along with wider and stronger out-of-band rejection compared to [8]. For proof-of-concept validation, a two-stage RF co-designed BPFI was synthesized

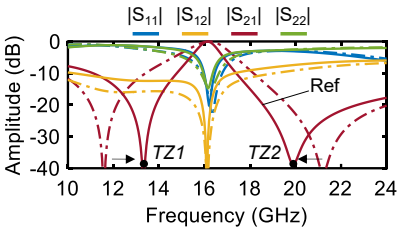


Fig. 2. UFS designs with different BW.

using a standardized coupled-resonator framework and experimentally validated at Ku-band.

II. Theoretical Foundations

A. TZ-Generating UFS

The circuit schematic and monolithic microwave integrated circuit (MMIC) implementation of the multi-resonant feedback-based UFS, using a commercially available 0.15-μm InGaAs process with a two-metal-layer stack, are shown in Fig. 1(a) and (b), respectively. The UFS [8] consists of two parallel RF signal branches: 1) a transistor-based branch in common-source configuration and reverse orientation, and 2) a capacitively-loaded multi-resonant feedback branch, which introduces one transmission pole and two TZs. As discussed in [8], when the two branches exhibit close amplitudes with a 180° phase difference and a zero phase sum at centre frequency (f_{cen}), constructive interference in the forward direction and destructive cancellation in the reverse direction can be realized, as depicted in Fig. 1(c).

To develop its transistor-based branch, a 2-finger E-mode pHEMT transistor (unit gate width of 25 μm, f_T =113 GHz) is employed, biased at V_g =0.57 V and V_d =2.6 V. To ensure stability and impedance matching, R_1-R_3 are incorporated, also L_t and C_t are added to fine-tune the amplitude and phase of the transistor path. The component values are subsequently optimized so that the transistor path exhibits approximately 0 dB amplitude and a 90° phase lead at f_{cen} [light-blue traces, Fig. 1(d)], forming the basis for constructive and destructive interference in conjunction with the feedback path. The feedback path, on the other hand, should provide a reverse phase relative to the transistor branch at f_{cen} to enable forward signal construction and reverse cancellation. To this end, a multi-resonant feedback network is employed, consisting of a multi-resonant cell (green block, Fig. 1(a)), two series transmission-line (TL) sections L_f and two series resistors R_a. The multi-resonant cell generates a transmission pole at 15.1 GHz (below f_{cen}) and two TZs located at 11.6 GHz (f_{TZ1}) and 21.3 GHz (f_{TZ2}), controlled by C_{f1} and C_{f2}, respectively. The L_f introduces an additional phase lag, facilitating the required ~−90° phase shift in the feedback path [purple traces, Fig. 1(d)], while resistors R_a help attenuate feedback for stability.

The MMIC layout implementation of the UFS, shown in Fig. 1(b), includes the detailed transistor biasing network, which is omitted from the idealized circuit schematic in Fig. 1(a). Inductors are connected in series within the biasing paths to properly bias the gate and the drain of the transistor, while resistors R_g and R_d are inserted in series to enhance transistor stability. Additionally, decoupling resistor–capacitor (RC) networks are connected in shunt within the biasing circuit to stabilize power supply voltages and reduce high-frequency noise. C_b is placed in series along the RF path to pass the RF signal while blocking DC bias leakage.

The component values of the UFS are optimized for good impedance matching and a reverse isolation greater than 40 dB at f_{cen}, and are listed in the caption of Fig. 1. Its circuit-simulated responses are shown in Fig. 1(c), where the forward transmission pole arises from the zero-phase loop formed between the feedback and transistor paths, while in the reverse direction, signal cancellation occurs due to the ~180° phase difference and amplitude balance between the two branches. Furthermore, at f_{TZ1} and f_{TZ2}, both the transistor and feedback paths exhibit near-zero transmission from P1 to P2, thereby forming two TZs in the forward response of the UFS. In addition, the UFS can be flexibly designed with different bandwidths (BWs) by asynchronously adjusting C_{f1} and C_{f2} in the multi-resonant cell. For example, decreasing C_{f1} while increasing C_{f2}, shifts f_{TZ1} upward and f_{TZ2} downward, resulting in a narrower passband, as illustrated in Fig. 2.

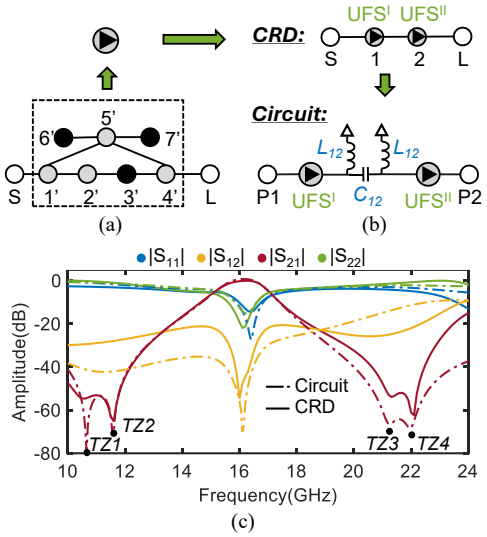


Fig. 3. (a) CRD of the UFS [8]. Two-stage BPFI: (b) CRD and its circuit implementation, and (c) comparison between circuit-simulated and CRD-synthesized responses. In the CRD of UFS^{I}: $m_{SI'}$ =1, $m_{4'L}$ =1, $m_{1'2'}$ =1, $m_{3'4'}$ =1.24, $m_{2'3'}$ =3.1-j1.28, $m_{3'2'}$ =0.27-j0.26, $m_{1'5'}$ =0.56, $m_{4'5'}$ =0.72, $m_{5'6'}$ =1.62, $m_{5'7'}$ =0.86, $m_{6'6'}$ =5.84, $m_{7'7'}$ =-4.9, $R_{1'1'}$ =-0.12-j1.32, $R_{2'2'}$ =1.08-j0.64, $R_{3'3'}$ =2-j0.64, $R_{4'4'}$ =0.2-j2.28. In the CRD of UFS^{II}: $m_{SI'}$ =1, $m_{4'L}$ =1, $m_{1'2'}$ =1.2, $m_{3'4'}$ =1.78, $m_{2'3'}$ =2.2-j2.58, $m_{3'2'}$ =0.51-j0.04, $m_{1'5'}$ =1, $m_{4'5'}$ =0.86, $m_{5'6'}$ =2.04, $m_{5'7'}$ =1.02, $m_{6'6'}$ =6.92, $m_{7'7'}$ =-5.2, $R_{1'1'}$ =0.6-j3.52, $R_{2'2'}$ =0.7-j0.71, $R_{3'3'}$ =1.48-j0.68, $R_{4'4'}$ =-0.09-j1.83. In the CRD of BPFI: m_{SI} =1, m_{12} =1, m_{2L} =1. In circuit implementation: C_{12} =0.2 pF, L_{12} =0.5 nH.

B. Co-Designed Quasi-Elliptic BPFI

Prior to the full filter synthesis, the coupling routing diagram (CRD) of a single UFS is designed as shown in Fig. 3(a). The transistor branch of the UFS is modelled by three non-resonating nodes (1', 2', 4') and one resonating node (3'), while the feedback path is represented by one non-resonating node (5') and two resonating nodes (6',7') as discussed in [8]. The self-coupling coefficients $m_{6'6'}$ and $m_{7'7'}$ determine the locations of the two TZs in the UFS response. For a two-stage BPFI composed of cascaded UFSs, the two UFSs (UFS^{I} and UFS^{II}) are intentionally designed with different TZ locations to broaden the out-of-band rejection. Specifically, TZs of UFS^{I} are located at 11.6 GHz (f_{TZ2}) and 21.3 GHz (f_{TZ3}), while those of UFS^{II} are located at 10.6 GHz (f_{TZ1}) and 22 GHz (f_{TZ4}). The coupling values in CRDs of both UFSs are calculated and optimized following the procedure in [8], with the final values provided in the caption of Fig. 3.

Based on the CRD of UFS, the two-stage BPFI prototype is analysed using coupled-resonator-based synthesis. Its CRD is illustrated at the top of Fig. 3(b), where the coupling values among the UFSs and the source/load nodes are also provided in the caption of Fig. 3. The corresponding synthesized S-parameters of the BPFI are shown in Fig. 3(c). The BPFI

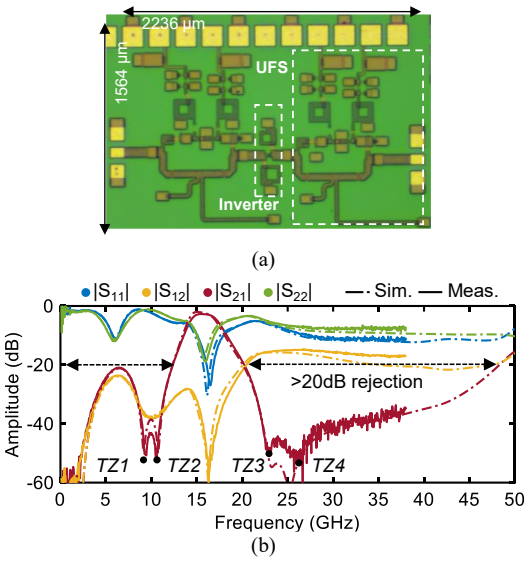


Fig. 4. Experimental validation of the BPFI. (a) Photograph. (b) Comparison of RF-measured and EM-simulated response.

circuit is then implemented with a f_{cen} of 16 GHz and a 3-dB fractional bandwidth (FBW) of 12%, as shown at the bottom of Fig. 3(b). The interstage coupling between the two UFSs is realized using a compact lumped-element high-pass π-network, with LC values calculated by (1).

$$C_{12} = \frac{m_{12}}{2\pi f_{cen} \times 50} \text{ F}, \; L_{12} = \frac{50}{2\pi f_{cen} \times m_{12}} \text{ H} \qquad (1)$$

where m_{12} is the coupling value between UFSs. The circuit-simulated responses of the co-designed filter align closely with the CRD-synthesized results, as shown in Fig. 3(c), validating the applicability of coupled-resonator-based synthesis from reciprocal filters to UFS-based configurations.

III. Experimental Validation

To validate the proposed concept, the two-stage BPFI prototype exhibiting a filtering response shaped by two poles and four TZs was manufactured using a 0.15 µm InGaAs process and characterized at Ku-band. On-wafer GSG-probed measurements were conducted using a PNA-X N5247B network analyser, with pads and probe effects de-embedded. A photograph of the manufactured chip is shown in Fig. 4(a). The measured RF responses, plotted over a wide frequency range in Fig. 4(b), closely agree with EM simulations. The BPFI exhibits a f_{cen} of 15.9 GHz with a 3-dB FBW of 20%. Four TZs are observed at 9.3, 10.6, 22.8, and 26 GHz, which contribute to wide out-of-band rejection. Additional suppression near DC is achieved through the use of a high-pass π-network between the two UFSs. With bias voltages of V_b =0.59 V and V_c =3.1 V for the first UFS, and V_b =0.64 V and V_c =3 V for the second UFS, the prototype achieves a gain of -2.7 dB, directivity of 60 dB, NF of 7.8 dB, and an input third-order intercept point (IIP3) of 8.7 dBm at f_{cen}. In addition, a wide stopband with greater than 20 dB rejection is maintained from DC to 12.3 GHz and from 20.1 to 48.3 GHz, based on simulated results that agree well with measurements up to 38 GHz (limited by probe bandwidth). Table I compares the proposed BPFI with state-of-the-art active MMIC unilateral components. Compared with the reference design in [8], the proposed architecture achieves higher directivity (60 dB vs. 20 dB) and more TZs (4 vs. 2) while using the same number of stages. Compared with other state-of-the-art, the proposed architecture exhibits wide upper stopband, the highest directivity and the largest number of TZs, while maintaining the lowest power consumption among designs implemented in the same technology.

TABLE I. Comparison with State-of-the-Art Active MMIC Unilateral Components

Ref.	[7]	[8]	[9]	[10]	**T.W.**
Tech.	GaAs	GaAs	GaAs	BiCMOS	GaAs
Freq. (GHz)	8.6	17.3~19.5	13	5.5	15.9
D (dB)	30.6	13~20	30	30	60
$\|S_{21}\|$ (dB)	−1.9	−3.9~−1.9	−1.7	−2	−2.7
N/TZs	5/0	2/2	4/2	N.A.	2/4
Ratio*	N.A.	N.A.	N.A.	N.A.	3[$]
NF (dB)	N.A.	5.9~7	9.2	13	7.8
IIP3 (dBm)	20.4	−4.2~10	0.2	0.7	8.7
P_{DC} (mW)	228.6	34	44	5.4	27
Size (λ×λ)	0.034×0.233	0.088×0.11	0.099×0.097	0.011×0.008	0.084×0.12
Filt.	Yes	Yes	Yes	No	Yes

D: directivity; N: number of transmission poles; Filt.: filtering capabilities.; *Ratio is defined as the ratio of the upper stopband frequency to the center frequency; [$]: simulated.

IV. Conclusion

This paper demonstrated a Ku-band GaAs MMIC quasi-elliptic BPFI design employing two cascaded UFSs to realize a transfer function with high directivity, high selectivity, wide and strong out-of-band rejection. Using a coupled-resonator-based synthesis, a two-stage BPFI prototype was designed and manufactured in a 0.15 µm GaAs process. It achieved 15.9 GHz f_{cen}, 20% 3-dB FBW, 60 dB directivity, and a wide stopband with greater than 20 dB rejection is maintained from DC to 12.4 GHz and from 20.1 to 50 GHz shaped by four TZs.

Acknowledgment

This work was supported by Research Ireland under grant 20/RP/8334. The authors would like to acknowledge WIN Semiconductors for manufacturing the devices.

References

[1] K. E. Kolodziej, B. T. Perry and J. S. Herd, "In-band full-duplex technology: techniques and systems survey," *IEEE Trans. Microw. Theory Techn.*, vol. 67, no. 7, pp. 3025-3041, July 2019.

[2] R. J. Cameron, C. M. Kudsia, and R. R. Mansour, *Microwave Filters for Communication Systems*. New York, NY, USA: Wiley, 2007.

[3] A. Ashley and D. Psychogiou, "Ferrite-based multi-port circulators with RF co-designed bandpass filtering capabilities," *IEEE Trans. Microw. Theory Techn.* , vol. 71, No. 6, pp. 2594–2605, January 2023.

[4] Z. Zhang and D. Psychogiou, "Incorporating directionality in transversal-resonator-based bandpass filters with tunable transfer function characteristics," *IEEE Trans. Circuits Syst. I, Reg. Papers*, vol. 70, no. 12, pp. 5194-5207, Dec. 2023.

[5] D. Simpson and D. Psychogiou, "MMIC active bandpass filter with nonreciprocal and quasi-elliptic response," *IEEE Microw. Wireless Technol. Lett.*, vol. 33, no. 2, pp. 141-144, Feb. 2023.

[6] A. Ashley and D. Psychogiou, "RF co-designed bandpass filters/isolators using nonreciprocal resonant stages and microwave resonators," *IEEE Trans. Microw. Theory Techn.*, vol. 69, no. 4, pp. 2178-2190, Apr. 2021.

[7] A. Ashley and D. Psychogiou, "MMIC GaAs isolators and quasi-circulators with co-designed RF filtering functionality," *IEEE J. Microw.*, vol. 3, no. 1, pp. 102-114, Jan. 2023.

[8] K. Li and D. Psychogiou, "Multiconfigurable RF codesigned GaAs MMIC filter/isolator/switch (FIS)," *IEEE Microw. Wireless Technol. Lett.*, doi: 10.1109/LMWT.2025.3614088.

[9] K. Li, A. Fontana and D. Psychogiou, "Ku-band multi-functional bandpass filtering isolators (BPFIs) using GaAs coupled-line-based unilateral frequency-selective stages," in *Proc. IEEE MTT-S Int. Microw. Symp. (IMS),* Jun, 2025, pp. 950-953.

[10] J. Lee, J. D. Cressler and A. J. Joseph, "A 5-6 GHz SiGe HBT monolithic active isolator for improving reverse isolation in wireless systems," *IEEE Microw. Wireless Compon. Lett.*, vol. 15, no. 4, pp. 220-222, Apr. 2005.